Therapeutic potential of dexamethasone Nano chitosan synthesized from chitosan as a novel treatment of pulmonary fibrosis in C57BL/6 mice

Afaf Hendawy Kamel, Eman Adel Hassanin Sherif, Waleed Khaled. El Zawawy & Nashwa Ahmed El-shinawy

Taylor & Francis
Taylor & Francis Group

Therapeutic potential of dexamethasone Nano chitosan synthesized from chitosan as a novel treatment of pulmonary fibrosis in C57BL/6 mice

Afaf Hendawy Kamel [a], Eman Adel Hassanin Sherif[a], Waleed Khaled. El Zawawy [b] and Nashwa Ahmed El-shinawy [c]

aDepartment of Zoology, Faculty of Women for Arts, Science and Education, Ain Shams University, Heliopolis, Cairo, Egypt; bDepartment of Chemical Industries Research Division, National Research Centre, Dokki, Giza, Egypt; cDepartment of Physiology, Zoology Department, Department of Women for Arts, Science and Education, Ain Shams University, Heliopolis, Cairo, Egypt

ABSTRACT

Back ground: Pulmonary fibrosis is an irreversible disease with excessive scarring and fibrosis of lung tissue. Glucocorticoid therapy of dexamethasone attenuates lung inflammation with severe adverse effects. Subsequently, synthesizing Nano chitosan from chitosan macromolecule and loading dexamethasone onto Nano chitosan particles have shown improved pharmacokinetics of dexamethasone. *Purpose:* The aim of this study was to prepare and characterize dexamethasone Nano chitosan particles chemically and then to evaluate the effectiveness of loading dexamethasone onto Nano chitosan as a treatment of pulmonary injury induced by bleomycin-induced in C57BL/6 mice. *Results:* This study elucidated significant elevations of serum malondialdehyde and lactate dehydrogenase with an increased lung tissue inflammatory mediators, collagen profile, Caspase-3, and MUC5AC gene expressions. This was accompanied by a significant elevation in total and differential leukocyte counts in bronchoalveolar lavage fluid. Besides, there were recognized histological and histopathological alterations in lung tissue sections following both 14 and 28 days of bleomycin instillation. Consequently, treatment of lung injury by dexamethasone alone or dexamethasone loaded onto Nano chitosan particles revealed a significant reduction of MDA and LDH, a decline in lung tissue inflammatory mediators, collagen profile, Caspase-3, and MUC5AC gene expressions. This was accompanied by a significant reduction in total and differential leukocyte counts in bronchoalveolar lavage fluid. However, loading dexamethasone onto Nano chitosan provided novel insights in pulmonary injury treatment

1. Introduction

Pulmonary fibrosis (PF) is the most common interstitial lung disease that affects over five million people worldwide. It leads to the replacement of healthy lung tissue by fibrous connective tissue [1]. Moreover, pulmonary fibrosis is characterized by the replacement of normal alveolar space by mesenchymal cells and extracellular matrix [2]. It is assumed that inflammatory cells enter the lung and together with resident lung cells release mediators that stimulate fibroblast proliferation and collagen deposition within the lung interstitium. In addition, PF affects lung gas exchange causing severe respiratory failure and death [3].

Bleomycin (BLM) is a chemotherapeutic agent of glycopeptide antibiotics that is clinically used for the management of many human malignancies [4]. However, intra-tracheal instillation of BLM in rodents is a well-established, widely accepted used model of lung fibrosis since it closely resembles the human fibrotic lung disease [5]. Inflammation and reactive oxygen species are important factors in bleomycin-induced pulmonary fibrosis, and inhibiting these factors might help in

attenuating the extent of the pulmonary disorder [6]. Hence, dexamethasone (DEX) is a synthetic well-known extensively used glucocorticoid with therapeutic activity in pulmonary diseases [7]. It is well documented that DEX attenuated BLM-induced lung fibrosis [8]. It has anti-inflammatory and immunosuppressive properties [9]. The main anti-inflammatory effect of dexamethasone is to inhibit a pro-inflammatory gene that encodes for chemokines, cytokines, cell adhesion molecules, and the acute inflammatory response [10]. In addition, DEX stabilizes the lysosomal membrane and prevents the release of proteolytic enzymes released during the inflammatory process [11]. However, DEX administration can cause several side effects either at high doses or after long-term use. Insulin resistance, hyperglycemia [12], weight change, hypertension, and hyperlipidemia are considered to be the primary adverse metabolic changes strongly associated with DEX treatment [13].

Therefore, new drugs with improved treatment efficacy and fewer side effects are urgently needed [14]. Nanomedicines can readily interact with

CONTACT Afaf Hendawy Kamel ✉ afaf.hendawy@women.asu.edu.eg 🏢 Department of Cytogenetics, Zoology Department of Faculty of Women for Arts, Science and Education, Ain Shams University, Asmaa Fahmy Street, Heliopolis, Cairo 11757, Egypt

biomolecules on both the cell surface and within the cell [15]. Nano chitosan (NCs) particles were considered as harmless polymer-carriers for the delivery of different various drugs [16].

The use of chitosan nanoparticles synthesized from chitosan as potential carriers for DEX sustained pulmonary drug delivery to the lungs and improved the pharmacological properties of the traditional drug dexamethasone diminishing its systemic side effects [17]. The smaller size of the drug-loaded on Nano chitosan allows it to extravasate from circulation where they can then deliver encapsulated dexamethasone to the lungs directly [18]. In addition, controlled release of the carried drug offered an effective way to optimize the bioavailability of the drug with minimal side effects [19].

The present study aims to prepare Nano chitosan particles from the biological macromolecule chitosan, then load dexamethasone on Nano chitosan particles. This was followed by chemical characterization of the novel dexamethasone Nano chitosan particles before and after loading with DEX to confirm the loading of DEX on Nano-chitosan particles. In addition, *in vivo* evaluation of the therapeutic effectiveness of loading dexamethasone on Nano chitosan particles as a novel modification compared to the traditional treatment by dexamethasone alone through decreases the side effects of bleomycin-induced pulmonary injury in mice model.

2. Materials

2.1. Chemicals Nano chitosan particles (NCs) as a carrier system for dexamethasone

Chitosan ($C_{56}H_{103}N_9O_{39}$) is a white powder that was purchased from Sigma-Aldrich, USA. Nano chitosan was prepared from Chitosan powder by dissolving 0.2 g of Chitosan in 100 ml acetic acid and sonicating for 15 minutes using Sonics Vibra Cell (Sonics &Materials Inc). It was then dried at room temperature and the sample was ground to fine powder according to the method of [20] (2009) and [21] et al. (2017). 0.1 g of Nano-chitosan was swelled in 3 ml distilled water and 3 ml ethanol (1:1, water: ethanol) for 30 minutes then loaded with 0.006 g of dexamethasone and left for drying at room temperature for 24 hours. Dose selection for DEX was based on the calculation of the equivalent human therapeutic dose [22].

2.2. Chemical characterization for the new compound (DEX-NCs)

2.2.1. Scanning electron microscope (SEM)

The surface morphology of the Nano chitosan with and without DEX was examined by scanning electron microscope (SEM) using JEOL JXA 840A electron microprobe analyzer [JOEL USA Inc, Peabody, MA, National Research Center (QUANTA FEG250)] on aluminum stubs and coated with a thin layer of palladium-gold alloy.

2.2.2. Transmission electron microscope (TEM)

A transmission electron microscope (TEM, JEOL-2100) operating at 200 kV with a resolution of 0.14 nm was specifically used to dedicate the shape and the particle size of Nano chitosan. 10-20µl of Nano chitosan was put in 50ml water: ethanol (1:3) and sonicated for 15 minutes, then removed from the solution by filtration and the samples of Nano chitosan before and after loading with DEX were examined under the transmission electron microscope.

2.2.3. Energy-dispersive X-ray analysis (EDXA)

Energy dispersive x-ray analysis was carried out to detect the elemental analysis and identify DEX and its loading on Nano chitosan samples

2.2.4. Fourier transform infrared spectroscopy (FTIR)

The chemical structural characteristics of Dexamethasone, Nano chitosan, and DEX-chitosan nanoparticles were investigated through Fourier transform infrared spectroscopy (FTIR spectra analysis). They were taken in KBr pellets using Jasco FT/IR 6100 instrument. Bands were recorded in the range of 4000-500 cm^{-1}.

2.3. In vivo animal studies and experimental design

Specific pathogen-free, 8–10 week old male C57BL/6 mice weighing 20–25 grams were purchased from the animal house of the Faculty of Agriculture, Alexandria University.They have housed in wire mesh laboratory animal cages. Each cage was provided with a mesh drawer for collecting and removing wastes which were done daily. Animals were kept under standard laboratory conditions (room temperature 20–25°C, 50–60% relative humidity, with natural day/night light cycle). Water and food were available *ad libitum*. Animals were allowed for 7 days as a pre-experimental period to adapt to the laboratory conditions. All animal procedures were performed following the guidelines for the care and use of experimental animals established by the Committee of the Purpose of Control and Supervision of Experiments on Animals (CPCSEA) and the National Institutes of Health (NIH) protocol approved by the Faculty of Agriculture, Alexandria University. A total number of 80 male C57BL/6 mice were divided into five groups each consisting of 16 animals. The first group served as the normal control (NC) group that received distilled water. The second group was the

dexamethasone (DEX) group that was injected intraperitoneally with dexamethasone at a dose of 0.45 mg/kg body weight/ day for 28 days. The third group served as the bleomycin (BLM) group that received a single intra-tracheal dose of 1 mg bleomycin/kg body weight. The fourth experimental group was the bleomycin group that received a single intra-tracheal dose of 1 mg bleomycin/kg body weight and then was treated with 0.45 mg/kg dexamethasone (BLM/DEX) for 28 days. The fifth group was the bleomycin group that received a single intra-tracheal dose of 1 mg bleomycin/kg body weight and then was treated with 0.45 mg/kg dexamethasone Nano chitosan particles (DEX-NCs) for 28 days. After 14 days 40 animals representing 8 mice) from each experimental group were dissected followed by another 40 animals after 28 days.

2.3.1. Blood sampling
After 14 days and 28 days, animals were autopsied through diethyl ether (Sigma, USA) inhalation anesthesia, after which animals were carefully dissected. Blood was collected by cardiac puncture in centrifuge tubes left to clot and centrifuged at 3000 rpm for 20 minutes.

2.3.2. Determination of serum lactate dehydrogenase and malondialdehyde
Serum was divided into small aliquots and stored at −20°C until analysis. Serum was then used for the determination of the Lactate dehydrogenase enzyme in serum according to the method of Caraway [23] and malondialdehyde content (MDA) according to the method of Kei [24]. Commercial kits were purchased from Randox, U.K

2.3.3. Tissue sampling
Animals were sacrificed lungs were immediately excised, washed with ice-cold saline. A part of each left lung was homogenized in phosphate buffer saline solution pH7.4 (10% w/v) with a homogenizer MPW-302 Poland. Lung homogenates were centrifuged at (4000 rpm at 4°C for 15 min). Supernatants were frozen at −80°C.

2.3.3.1. Inflammatory mediators. Lung homogenates were used for the determination of mice Tumor Necrosis Factor- α (TNF-α, Transforming Growth Factor β1 (TGF-β1), Nuclear Factor (NFκB), and Matrix Metalloproteinase 2 enzyme (MMP-2) levels. They were performed according to the manufacturer's instructions by ELISA (Sandwich Immunoassay Technique) using commercial kits purchased from MyBio Source Company USA.

2.3.3.2. Collagen profile tests. Lung homogenates were used for the determination of mice hydroxyproline assay and collagen type 1 α by quantitative sandwich enzyme immunoassay technique which was purchased from MyBio Source Company, USA.

2.3.3.3. Gene expression of Caspase-3, BCL2, and MUC5AC genes in lung tissue by quantitative real-time polymerase chain reaction (QRT-PCR).
Total RNA was extracted from lung tissue using a Qiagen tissue extraction kit (Qiagen, USA) according to the manufacturer's instructions. The purity of obtained RNA was verified spectrophotometrically at 260 nm. The extracted RNA was reverse transcribed into cDNA using an RT-PCR kit (Fermentas USA) according to the manufacturer's instructions.

To assess the expression of Caspase-3, BCL2, and MUC5AC genes, quantitative real-time PCR was performed using SYBR Green PCR Master Mix (Qiagen, Germany) as described by the manufacturer.

Briefly, 12.5 μL of QuntiFast SYBR Green PCR Master Mix, 5.5 μL dH2O, 2 μL primer pair mix (1/μLeach primer), and 5 μL cDNA in a final reaction volume of 25μL. The sequences of primers were:

Caspase 3: Forward 5′- TGTCATCTCGCTCTGGTA CG –3′

Reverse 5′- AAATGACCCCTTCATCACCA-3′

BCL2: Forward5′- GAGAGCGTCAACAGGGAGA TG-3′

Reverse5′- CCAGCCTCCGTTATCCTGGA –3′

MUC5AC: Forward5′-ATCACCATCTTCCAGGA GCG-3′

Reverse5′-CCTGCTTCACCACCTTCTTG-3′

β-actin: Forward5′-GGTCGGTGTGAACGGAT TTGG-3′

Reverse 5′- ATGTAGGCCATGAGGTCCACC –3′

PCR reactions included 10 min at 95°C for activation of Ampli Taq DNA polymerase, followed by 40 cycles at 95 °C for 15 seconds (denaturing) and 60 °C for 1 min (annealing and extension). The data were expressed in cycle threshold (C_t) where the increased fluorescence curve passes across a threshold value. Relative gene expression was calculated as 2 −ΔΔCt and was normalized to β-actin [25].

2.3.4 Total and differential leukocyte counts in bronchoalveolar Lavage (BAL) fluid
After anesthesia, mice were fixed on the desk. BAL fluid was collected by the injection of 3 mL saline three times, followed by mild aspiration of the fluid from the lungs after securing an intratracheal catheter within the trachea. Then the fluid was centrifuged at 1500 rpm for 10 minutes [26]. The total numbers of leukocytes (macrophages, lymphocytes, and neutrophils) in the BAL fluid,

cell pellets were re-suspended in 20 µl of Bovine albumin serum, then stained by Giemsa stain, counted (200 cells/slide) in a hemocytometer using morphological criteria under a light microscope. Differential cell counts were obtained from a count of 200 cells per smear [27].

2.3.5. Histological investigations

After 14 and 28 days, apart from the right lung of each mice/group was fixed in 10% formalin–saline and processed for histological examination by using Hematoxylin and Eosin stain (H&E) [28].

2.3.6. Histopathological investigations and grades of pulmonary injury

The grades of pulmonary inflammation and fibrosis in lung tissue sections were analyzed by Masson Trichrome staining to identify collagen fibers [29]. The scoring system was used to estimate the severity of pulmonary injury on a numerical scale. Using a 10X objective, an average of 10 fields per slide were assessed for lung injury severity after 14 and 28 days. Each field was assigned a score between 0 and 8 (total fibrosis). The rating criteria were as follows: 0 = normal lung, 1 = minimal fibrous thickening of bronchiolar or alveolar wall, 3 = moderate thickening of walls without damage to lung architecture, 4 and 5 = increased fibrosis with damage to lung structure and formation of fibrous bands, 6 and 7 = severe distortion of the structure and large fibrous areas, 8 = total fibrous obliteration of the field [30]. The mean of the scores for all fields was taken as the fibrotic score of the section [31].

2.4. Statistical analysis

Data were expressed as means ± standard error of means (SE). All the recorded data were analyzed using the Statistical Package for Social Sciences (SPSS) version 10 computer program. The significance of differences between means of the control and all treated mice (*) and the significance of differences between means of bleomycin treated groups and bleomycin group (#) were evaluated by one-way analysis of variance (ANOVA) test. The values of $p < 0.05$ were considered statistically significant.

3. Results

3.1. Chemical characterization

3.1.1. Scanning electron microscopy (SEM)

SEM of chitosan nanoparticles before loading with dexamethasone showed that NCs appeared like particles at 3000x with a diameter ranging from 2.05 up to 5.07 µm with irregular spherical structure at the cross-section (Figure 1a). While scanning electron microscopy of dexamethasone-Nano chitosan (DEX-NCs) at a higher power of 30000 x showed the spherical

shape of dexamethasone with a diameter ranging from 2.188 and 3.005 µm adsorbed on the surface and absorbed inside Nano-chitosan particles as showed in Figure 1b.

3.1.2. Transmission electron microscope (TEM)

TEM of Nano-chitosan before loading with dexamethasone showed that the particle size of Nano-chitosan was about 200 nm (Figure 2a). TEM of DEX- NCs particles revealed that DEX was adsorbed at the surface of Nano-chitosan particles (Figure 2b).

3.1.3. Energy-dispersive X-ray analysis and drug loading (EDX)

Loading DEX onto NCs-particles was confirmed by using the EDX analysis Figure 3(a,Figure 3b,Figure 3c), and Table 1. Table 1 illustrated the presence of Florine (F) which is one of the DEX components with a weight % of 0.55 in the EDX of DEX alone. Conversely, the EDX analysis of NCs–particles alone showed no Florine in its structure.

On the other hand, studying the EDX of DEX-NCs particles confirmed the presence of Florine in its structure with a weight % of 0.42 indicating that the particles of the drug were adsorbed on the surface of the NCs particles and absorbed into the NCsparticles. Also, the weight % of carbon content elevated from 13.73 in NCs to 19.27 in to prove that DEX was loaded onto the NCsparticles. After loading the drug onto
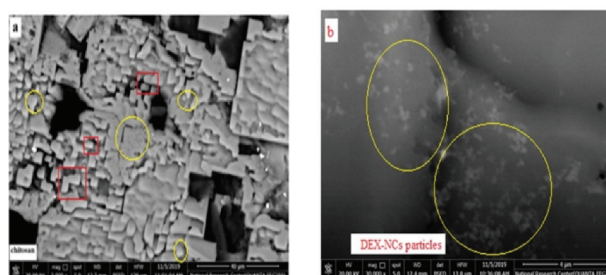
Figure 1. SEM of chitosan nanoparticles before loading with dexamethasone at 3000x (Figure 1a) and dexamethasone-Nano chitosan (DEX-NCs) particles at higher power of 30,000 x (Figure 1b) in cross-section.
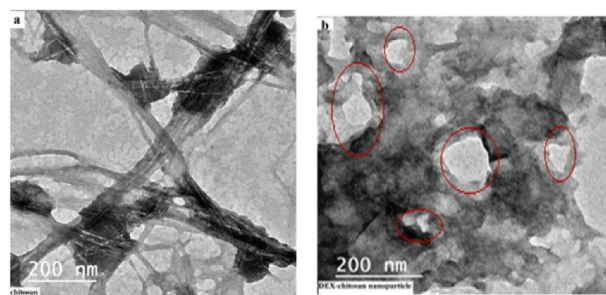
Figure 2. TEM of Nano-chitosan before loading with dexamethasone with particle size 200 nm (Figure 2a). TEM of DEX-NCs particles (Figure 2b).
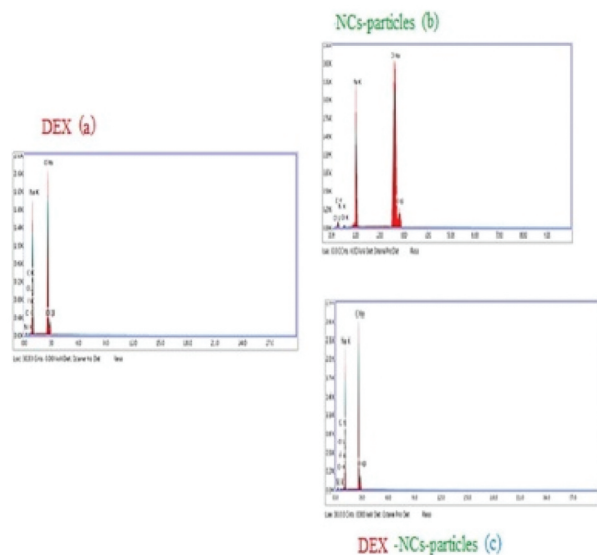
Figure 3. EDX of DEX (Figure 3a), NCs (Figure 3b), and DEX-NCs particles (Figure 3c).

Table 1. Weight % of carbon, nitrogen, oxygen, sodium, chlorine, and florine in DEX, NCs particles and DEX-NCs .

|	Weight%		
Element	DEX	NCs	DEX-NCs
Carbon	13.89.	13.73	19.40
Nitrogen	–	0.28	0.39
Oxygen	2.19	2.63	2.67
Sodium	37.15	37.12	35.34
Chlorine	46.22	46.24	41.78
Florine	0.55	-	0.42

DEX: Dexamethasone.
NCs: nano chitosan.
DEX-NCs: Dexamethasone nano chitosan.

NCs particles, the weight % of the nitrogen content of NCs particles was increased from 0.28 to 0.39 in DEX-NCs particles.

3.1.4. Fourier transform infrared spectroscopy (FTIR)

FTIR of DEX, NCs, and DEX-NCs are displayed in Figure 4 which shows the main peaks of NCs that can be assigned as follows: 3456 cm^{-1} (N–H and O–H stretching vibration), 2925 cm^{-1} (CH symmetric stretch), 1616 cm^{-1} (C = O stretching vibration), 1438 cm^{-1} (C–N stretching vibration), 1363 cm^{-1} (CH bending vibration), 1170 cm^{-1} (C–O–C bending vibration), and 1073 cm^{-1} (C–OH stretching vibration).

For DEX, there was a very strong and sharp peak at 3471 cm^{-1} (O-H stretching vibration) and peak at 2948 cm^{-1} represented stretching vibration of C-H, and peak at 1704 cm^{-1} that was assigned to C = O. The peaks at 1662 cm^{-1} and 1616 cm^{-1} represented the stretching vibration of the C = C bond. On the other hand, there was broadband at 3459 cm^{-1} for each NCs, and DEX-NCs particles characterized O-H stretching
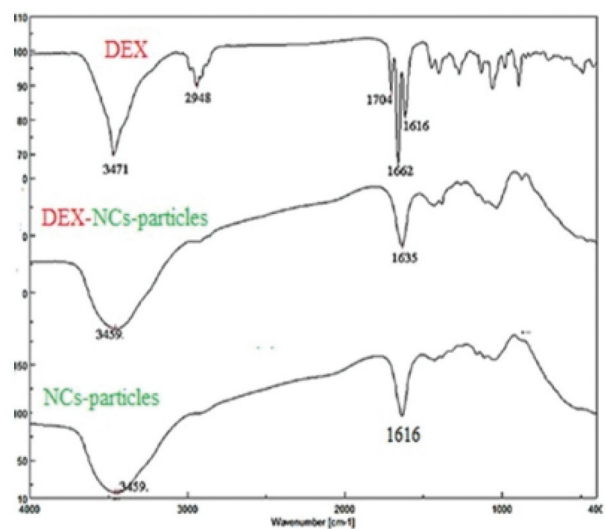
Figure 4. FT-IR Spectroscopy of DEX (Figure 4a), NCs (Figure 4b), and DEX-NCs (Figure 4c) particles.

vibration. The sharp band and strong sharp peak at 1635 cm^{-1} and 1616 cm^{-1} represented stretching vibration of the C = O group of NCs and DEX-NCs particles (Figure 4).

3.2. In vivo animal studies

3.2.1. Determination of LDH and MDA in serum
A significant increase in LDH and MDA levels was confirmed after 14 and 28 days of BLM induction when compared with the NC group. DEX administration to BLM treated mice recorded a 1.45 and 2.92 fold decrease in LDH activities after 14 and 28 days, respectively. On the other hand, DEX-NCs treatment showed a decline of 1.78 and 3.69 folds when compared with the BLM group (Table 2). Likewise, a significant increase ($P < 0.05$) in serum MDA levels was recorded either after 14 or 28 days of experimental study when compared to the BLM treated group. Treatment of BLM group with DEX loaded on NCs particles signified a decline ($p < 0.05$) in the mean values of serum MDA to record a 2.98 fold decrease after 28 days when compared to BLM group (Table 2).

3.2.2. Inflammatory mediators
Table 3 presents a significant increase ($P < 0.05$) in inflammatory mediators of TNF-α, TGF-β1, NFκB, and MMP2 levels in lung tissue after 14 days of intratracheal BLM instillation. The increase in these lung parameters progressed until 28 days of the experimental study period in the BLM group when compared to the NC group. Quite the opposite, statistically ameliorated results ($p < .005$) in the levels of these cytokines and lung tissue inflammatory marker MMP2 were recorded in BLM/DEX and BLM/DEX-NCs groups compared to BLM. The most ameliorated results in all investigated inflammatory mediators were

Table 2. Levels of serum LDH and MDA in different experimental groups.

Parameter	Duration	Control groups		Bleomycin groups		
		NC	DEX	BLM	BLM/DEX	BLM/DEX-NCs
LDH (U/L)	14 days	129.99 ± 7.4	153.9 ± 7.24	470.64*±12.5	324.42*#±3.78	161.26*#±8.9
	28 days	130.11 ± 7.83	147.6 ± 7.06	573.12*±2.03	321.47*#±8.60	144.67#±1.34
MDA (nmol/ml)	14 days	73.26 ± 2.01	88.00 ± 5.0	169.21*±1.37	124*#±4.11	93.32*#±4.41
	28 days	75.45 ± 2.77	85.4 ± 1.72	237.3*±1.49	118.6*#±2.78	79.72#±3.31

Normal Control DEX: Dexamethasone BLM: Bleomycin BLM/DEX: Bleomycin+Dexamethasone.
BLM/DEX-NCs: Bleomycin+Dexamethasone nano chitosan.
*Significant change at $P < 0.05$ of all experimental groups in comparison with NC group.
#Significant change at $P < 0.05$ of all BLM treated groups in comparison with BLM group.

Table 3. Inflammatory mediators (TNF-α, TGF-β1, NFκB, and MMP2) in lung tissue in different experimental groups.

Parameter	Duration	Control groups		Bleomycin groups		
		NC	DEX	BLM	BLM/DEX	BLM/DEX-NCs
TNF -α (Pg/ml)	14 days	14.43 ± 0.10	12.95 ± 0.23	89.36*±2.80	73.21*#±0.54	35.06*#±1.38
	28 days	13.65 ± 0.05	12.53 ± 0.06	127.2*±1.81	51.30*#±0.73	33.22*#±1.11
TGF-β (pg/ml)	14 days	26.05 ± 0.3	28.28 ± 1.15	77.51*±5.78	70.82*±2.69	50.94*#±0.86
	28 days	32.88 ± 0.14	28.01 ± 0.36	132.81*±0.84	53.24*#±5.70	38.15#±0.62
NF kB (pg/ml)	14 days	65.20 ± 0.06	59.5 ± 0.42	149.99*±2.82	98.61*#±3.96	77.96*#±1.36
	28 days	62.56 ± 0.16	60.04 ± 0.20	190.11*±1.94	95.22*#±0.64	62.88#±2.11
MMP2 (ng/ml)	14 days	2.08 ± 0.03	1.65 ± 0.07	7.17*±0.25	6.35*#±0.35	4.07*#±0.19
	28 days	2.27 ± 0.01	1.91 ± 0.03	14.32*±0.20	3.12*#±0.33	2.33#±0.07

Normal Control DEX: Dexamethasone BLM: Bleomycin BLM/DEX: Bleomycin+Dexamethasone.
BLM/DEX-NCs: Bleomycin+Dexamethasone nano chitosan.
* Significant change at $P < 0.05$ of all experimental groups in comparison with NC group.
# Significant change at $P < 0.05$ of all BLM treated groups in comparison with BLM group.

recorded after 28 days in DEX-NCs group to reveal 3.83, 3.48, 3.03 and 6.15 folds decline in TNF-α, TGF-β1, NFκB and MMP2 levels in lung, respectively (Table 3).

3.2.3. Collagen profile tests

Hydroxyproline content and collagen 1α in lung homogenate recorded a significant $(P < 0.05)$ elevation in their mean values in BLM treated animals compared to the NC group. On the contrary, treatment with DEX loaded on NCsparticles for 28 days to BLM group caused a significant decline $(p < 0.05)$ in the mean values of lung tissue hydroxyproline and collagen 1α to record (6.02 ± 0.26 and 81.00 ± 1.96) against BLM group of (29.15 ± 2.22 and 192.83 ± 6.19), respectively (Table 4).

3.2.4. Gene expression of Caspase-3, BCL2, and MUC5AC genes in lung tissue

BLM installation was associated with a significant $(P < 0.05)$ increase in Caspase-3 and MUC5AC gene expressions in lung tissue homogenates. This was accompanied by a profound decrease in BCL-2 gene expression after 14 and 28 days when compared to the NC group.

In contrast, a significant $(P < 0.05)$ decline in the gene expression of Caspase-3 and MUC5AC genes with a significant increase in BCL2 gene in lung tissue was observed after treatment with DEX or DEX loaded on NCs particles when compared to BLM group after either 14 or 28 days as illustrated in Table 5. It is worth mentioning that the most ameliorated results in all pre-mentioned parameters were observed after 28 days of treatment of DEX loaded on NCs particles to PF mice (Table 5).

Table 4. Collagen profile (Hydroxyproline and collagen 1α) in lung tissue in different experimental groups.

Parameter	Duration	Control groups		Bleomycin groups		
		NC	DEX	BLM	BLM/DEX	BLM/DEX-NCs
Hydroxyproline (ng/ml)	14 days	4.75 ± 0.05	3.63 ± 0.05	16.55*±1.07	13.4*#±0.22	7.96*#±0.27
	28 days	4.08 ± 0.03	4.02 ± 0.05	29.15*±2.22	9.21*#±0.46	6.02#±0.26
Collagen 1 α (ng/ml)	14 days	78.12 ± 0.07	77.00 ± 0.47	162.14*±2.84	125.88*#±1.93	89.28*#±2.19
	28 days	75.76 ± 0.18	74.63 ± 0.23	192.83*±6.19	100.33*#±2.93	81#±1.96

Normal Control DEX: Dexamethasone BLM: Bleomycin BLM/DEX: Bleomycin+Dexamethasone.
BLM/DEX-NCs: Bleomycin+Dexamethasone nano chitosan.
* Significant change at $P < 0.05$ of all experimental groups in comparison with NC group.
# Significant change at $P < 0.05$ of all BLM treated groups in comparison with BLM group.

Table 5. Relative quantification expression of (Caspase −3, MUC5AC, and BCL2) genes in lung tissue in different experimental groups.

		Control groups		Bleomycin groups		
Parameter	Duration	NC	DEX	BLM	BLM/DEX	BLM/DEX-NCs
Caspase −3	14 days	1.01 ± 0.01	0.85 ± 0.006	5.58*±0.40	5.03*±0.33	2.76*#±0.08
	28 days	1.01 ± 0.01	0.80 ± 0.01	10.33*±0.80	2.54*#±0.13	1.74#±0.10
Muc5 ac	14 days	1.01 ± 0.01	0.85 ± 0.006	5.58*±0.40	5.03*±0.33	2.76*#±0.08
	28 days	1.01 ± 0.01	0.80 ± 0.01	10.33*±0.80	2.54*#±0.13	1.74#±0.10
BCL2	14 days	1.01 ± 0.01	1.08 ± 0.04	0.22*±0.044	0.51*#±0.01	0.88*#±0.008
	28 days	1.00 ± 0.003	1.02 ± 0.006	0.13*±0.008	0.60*#±0.03	0.90*#±0.01

Normal Control DEX: Dexamethasone BLM: Bleomycin BLM/DEX: Bleomycin+Dexamethasone.
BLM/DEX-NCs: Bleomycin+Dexamethasone nano chitosan.
* Significant change at $P < 0.05$ of all experimental groups in comparison with NC group.
# Significant change at $P < 0.05$ of all BLM treated groups in comparison with BLM group.

Table 6. Total and differential leukocyte counts in BAL fluid in different experimental groups.

		Control groups		Bleomycin groups		
Parameter	Duration	NC	DEX	BLM	BLM/DEX	BLM/DEX-NCs
Total leukocytes ×10^6/ml	14 days	0.57 ± 0.03	1.12 ± 0.2	2.62*±0.26	2.51*±0.18	1.45*#±0.11
	28 days	0.68 ± 0.05	0.89 ± 0.03	3.41*±0.15	1.42*#±0.07	0.76#±0.03
Macrophages × 10^5/ml	14 days	3.16 ± 0.47	5.0 ± 0.00	17.0*±2.25	9.85*#±0.63	5.66#±0.42
	28 days	3.75 ± 0.17	4.69 ± 0.40	25.0*±1.25	8.14*#±1.16	4.83#±0.30
lymphocytes× 10^5/ml	14 days	2.33 ± 0.42	4.0 ± 0.42	11.87*±0.98	9.85*#±0.50	3.33#±0.42
	28 days	2.66 ± 0.42	3.5 ± 0.31	12.1*±0.74	6.0*#±0.92	3.00#±0.25
Neutrophils× 10^5/ml	14 days	2.16 ± 0.30	3.0 ± 0.44	6.37*±1.05	4.57*±0.97	2.0#±0.36
	28 days	1.83 ± 0.30	2.9 ± 0.33	6.87*±0.61	3.85*#±0.50	1.66#±0.33

Normal Control DEX: Dexamethasone BLM: Bleomycin BLM/DEX: Bleomycin+Dexamethasone.
BLM/DEX-NCs: Bleomycin+Dexamethasone nano chitosan.
* Significant change at $P < 0.05$ of all experimental groups in comparison with NC group.
# Significant change at $P < 0.05$ of all BLM treated groups in comparison with BLM group.
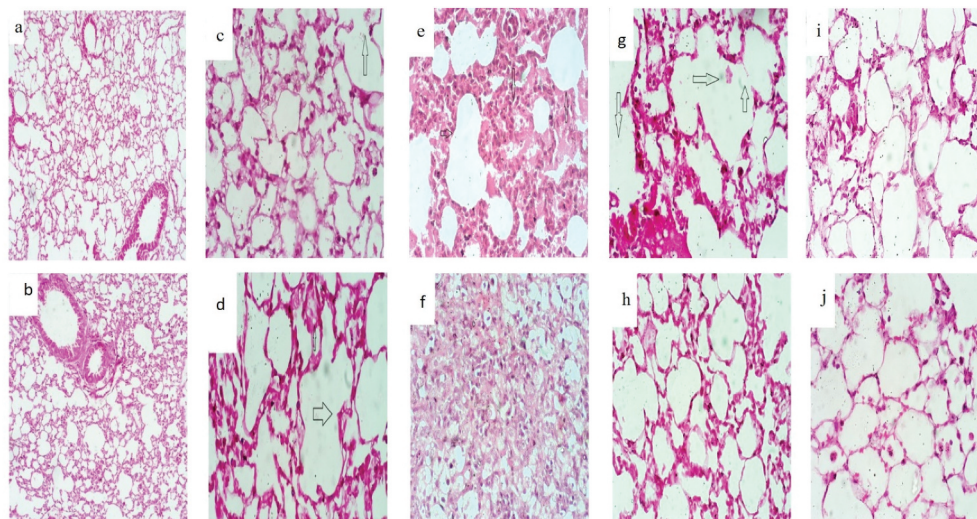
Figure 5. Photomicrograph of lung section (H&E x400) from normal control group after 14 (Figure 5a) and 28 days (Figure 5b). Lung section from Dexamethasone group after 14 days showed normal architecture with simple rupture of alveolar sacs ⇧ (Figure 5c). But after 28 days, there was increased rupture of some alveolar sacs that showed some ⇨ signs of edema (Figure 5d). Lung section of BLM group after 14 days ⇩ showing extensive damage of the lung tissue with distorted lung morphologies: collapsed alveolar spaces with inflammatory exudates wider and thickened interalveolar septa (Figure 5e). After 28 days, there was loss of the normal alveolar architecture and majority of the alveolar walls were occupied by collagenous fibers with diffused cellular infiltration (Figure 5f). BLM and DEX group after 14 days showed more rupture of alveolar walls ⇨ and excess of hyaline material (Figure 5g). After 28 days BLM and DEX showed restored normal tissue, slight thickening, and space expansion, mild edema of the interstitium and alveolar spaces with clear terminal (Figure 5h). Treatment with BLM/DEX-NCs for 14 days showed normal lung architecture with thin walls of alveolar sacs and decrease the inflammatory infiltration and improve lung function (Figure 5i). After 28 days, there was more improvement in walls of alveolar sacs, decreased inflammatory infiltration and improved lung structure (Figure 5) (H&E;x400).

3.2.5. Total and differential leukocyte counts in bronchoalveolar lavage (BAL) fluid

The results of Table 6 validate a significant *(P < 0.05)* 5 fold increase in total leukocytes with subsequent increased inflammatory cell counts of 6.66 fold in macrophages, 4.55 fold in lymphocytes, and 3.75 fold in neutrophils in BAL fluid after 28 days of BLM induction when compared to NC group. In addition, the total leukocyte counts and the differential counts of macrophage, lymphocytes, and neutrophils in BAL fluid revealed a significant *(P < 0.05)* reduction in BLM treated groups with DEX and DEX loaded on NCs particles after either 14 or 28 days.

3.2.6. Histological and histopathological investigations

Microscopically, lung sections stained with H&E of NC groups either for 14 days (Figure 5a) or 28 days (Figure 5b) revealed normal pulmonary architecture with a normal spongy appearance, clear alveolar cavities, and normal alveolar ducts. The interalveolar septa were formed from the epithelial tissue around the alveoli. Also, the microscopic observation of lungs treated with dexamethasone for 14 days (Figure 5c) demonstrated normal architecture with simple rupture of alveolar sacs. But after 28 days there was increased rupture of some alveolar sacs that showed some signs of edema (Figure 5d). Histological examination of lung sections stained by H&E of BLM treated mice for 14 days showed extensive damage of the lung tissue with distorted lung morphologies including collapsed alveolar spaces with inflammatory exudates, wider and thickened interalveolar septa (Figure 5e). This damage continued for 28 days to reveal a loss of normal alveolar architecture. In addition, the majority of the alveolar walls were occupied by collagenous fibers with diffuse cellular infiltration of macrophages and fibroblast as shown in Figure 5f.

Animals' lung sections treated with both BLM and DEX for 14 days elucidated more rupture of alveolar walls and excess of hyaline material as shown in Figure 5g.

Moreover, this study clarified that lung sections of BLM animals treated with DEX for 28 days showed slight thickening, space expansion, and mild edema of the interstitium and alveolar spaces with clear terminal bronchioles. Nevertheless, there was still congestion of the interalveolar septa with scattered inflammatory cells (Figure 5h). Lung tissue sections of the BLM/DEX-NCs group exhibited more improvement in lung architecture for 14 and 28 days to demonstrate more ameliorated histological features clarified as normal lung architecture with thin alveolar sacs walls and decreased inflammatory infiltration (Figure 5(i),Figure 5(j))Figure 5 (h,Figure 5e).jpg

3.2.7. Grades of pulmonary injury

According to the scoring system that was used to estimate the severity of pulmonary injury on a numerical scale, the grades of pulmonary inflammation and fibrosis in lung tissue sections were analyzed by Masson staining to identify collagen fibers.
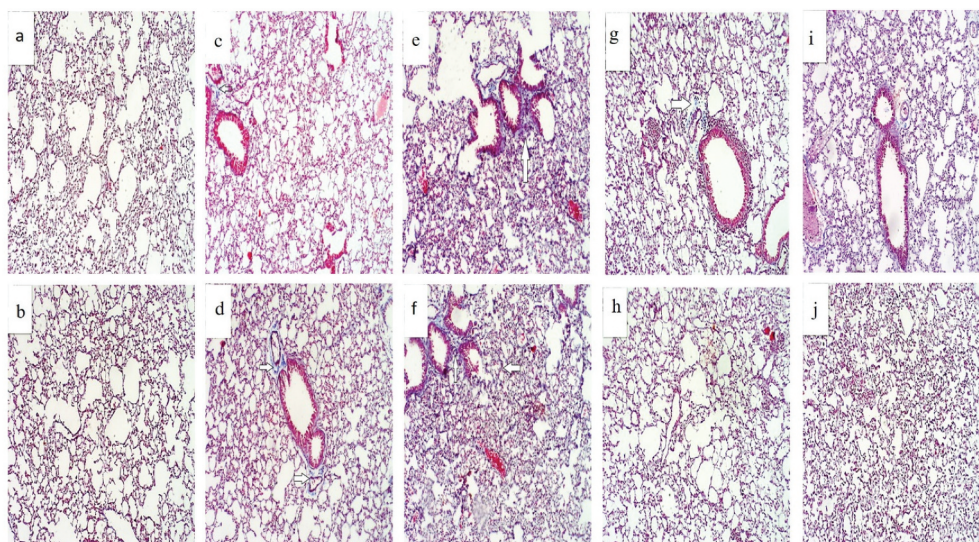
Figure 6. Photomicrograph of lung section (Masson's trichrome; x100) from normal control group showing normal alveolar structure with no collagenous fibers (grade 0) of fibrosis (Figure 6(a,b)). Lung section from DEX group after 14 days showing grade 2 fibrosis representing presence of simple collagenous fibers (Figure 6c). DEX group after 28 days showed (grade 1) of fibrosis with the presence of some collagenous fibers (Figure 6d). Lung section from BLM group after 14 days showed grade 7 of fibrosis with the presence of excess collagenous fibers (Figure 6e). BLM group after 28 days showed grade 8 of fibrosis with the presence of excess collagenous fibers (Figure 6f). BLM group treated DEX showing grade 4 of fibrosis after 14 days with the presence of collagenous fibeis (Figure 6g). BLM group treated with DEX for 28 days showed grade 3 of fibrosis with decreased collagenous fibers (Figure 6h). BLM group treated with DEX-NCs for 14 days showed grade 4 of fibrosis with some collagenous fibers (Figure 6), BLM/DEX-NCs for 28 days showed grade 3 of fibrosis with decreased collagenous fibers (Figure 6j) (Masson's trichrome; x100).

In Figure 6(a,Figure 6b), lung tissue sections stained by Masson's trichrome of NC group at 14 and 28 days showed grade (0) fibrosis where lung structure showed a normal pattern, normal alveolar septa with no burden at the most flimsy small fibers in some alveolar walls.

While DEX administration to animals for 14 days exhibited grade (2) fibrosis. Alveolar septa showed fibrotic changes with knot-like formation but were not connected. The alveoli were partly enlarged and rarefied with no fibrotic masses (Figure 6c). The fibrosis degree decreased to grade (1) by concurrent administration of DEX for 28 days to show isolated gentle fibrotic changes in alveolar septa. Alveoli were partly enlarged with no present fibrotic masses (Figure 6d).

Lung tissue sections of animals treated with BLM for 14 days showed grade (7) fibrosis in which alveolar septa were non-existent. Alveoli were obliterated with fibrous masses but still up to five air bubbles (Figure 6e). This fibrosis degree increased to reach grade (8) after 28 days of BLM installation in which alveolar septa were still non-existent and lung structure showed complete obliteration with presented fibrotic masses (Figure 6f).

After 14 days of experimental study, lung sections of BLM/DEX and BLM/DEX-NCs groups showed grade (4) fibrosis in which alveolar septa were variable with fibrotic masses (Figure 6(g,Figure 6i), respectively). But, following 28 days of experimental study, this fibrosis degree decreased to grade (3) in both pre-mentioned groups in which alveolar septa exhibited contiguous fibrotic walls predominantly in the whole microscopic field. The lung structure and the alveoli were partly enlarged and rarefied with no fibrotic masses as shown in Figure 6(h,Figure 6j).

4. Discussion

Pulmonary fibrosis (PF) is a multifactorial, chronic disease featured by the progressive formation of a scar in the lung parenchyma [32]. The lungs' fibrotic reaction is an irreversible process that is characterized by an increased fibroblast population with an intense and complex change in extracellular matrix turnover [33,34].

DEX is a very well-known widely available and cheap drug that plays an important role in attenuating BLM-induced lung fibrosis in mice [35,36].

Nevertheless, the application of DEX in PF was always under debate because PF implies a long treatment time. In addition, the high and frequent dose of DEX might cause many side effects [13]. Therefore, strategies to attenuate the accumulation and therapeutic index of DEX in lung tissue have been diminished by loading DEX on Nanoscaled carriers [37,38] giving them promising applications in medicine [39].

In this study, DEX was loaded on NCs polymeric matrix that was synthesized from chitosan. NCs particles were considered as a harmless polymer to be

used in the development of Nanocarriers for drug delivery [40]. NCs also possess potential therapeutic applications due to their biodegradability, biocompatibility, bioadhesive, and antibacterial performance [41].

When DEX was loaded on NCs particles, the SEM of (DEX-NCs) at 30000x confirmed that DEX had a spherical shape with a diameter of 2.188 and 3.005 μm and it was embedded inside NCs particles. These results were in accordance with **Ghadi et al.** [19] who verified that the absorption and bioavailability of drugs encapsulated into chitosan nanoparticles can be improved. Moreover, they can protect the delivered drugs effectively from enzyme degradation in vivo. Also, Nano chitosan carriers can improve DNA and drug bioavailability, resistance in vivo, enhance controlled sustained drug release by reducing drug toxicity. The smaller particle size of NCs seemed to have efficient interfacial interaction with the cell membrane facilitating endocytosis [19].

The animal study results revealed significantly increased levels of serum LDH and MDA in the BLM group when compared to the NC group. Any elevation in LDH activity can be considered as a significant index for the diagnosis of lung diseases. In addition, BLM treatment-induced reactive oxygen species in lung tissues lead to the increase in lipid peroxidation, which in turn-induced inflammation with decreased lung function [42].

The increased activities of LDH might be attributed to increased lipid peroxidation products like MDA in cellular membranes that produced marked alterations in the molecular organization of lipids resulting in increased membrane permeability and leakage of cytoplasmic markers into circulation [43].

These results were in line with the outcomes of the present investigation, which elucidated the elevations in lung tissue hydroxyproline and collagen 1 α content with subsequent significant elevations of TNF-α, TGF-β1, NFκB, and MMP2 after 14 days of intratracheal BLM instillation. The increase in these lung parameters progressed until 28 days of the experimental study period in the BLM group when compared to the NC group. In addition, the results of the present study validated the significant increase of total leukocytes with increased cell counts of neutrophils lymphocytes, and macrophages in BALF after both 14 and 28 days of BLM induction. Macrophages and neutrophils have also been documented to play role in lung parenchymal injury by releasing harmful free radicals and various proteolytic factors [44].

Furthermore, BLM stimulates alveolar macrophages to release inflammatory mediators. Elevated inflammatory infiltration in lung tissue and bronchoalveolar lavage fluid following BLM administration resulted in the deposition of collagen into the lung epithelial cells [44].

Damage and activation of alveolar epithelial cells may result in the release of TGF-β1, NFκB, and TNF-α that stimulated proliferation and accumulation of fibroblasts and deposition of a pathologic extracellular matrix [45]. Hydroxyproline induced pro-fibrotic proteins synthesized by transdifferentiation of fibroblasts into myoblasts and therefore increased levels of collagen I expression [46]. The extra deposition of hydroxyproline and its marker type I collagen in the form of extracellular matrix reflects the distortion and destruction of alveolar structures and loss of lung function [47] which in turn affected the efficiency of gas exchange across this membrane [4].

Additionally, MMP2 is capable of upregulating the pro-fibrotic mediators, downregulating the anti-fibrotic mediators, and enhancing cell migration [48] thus MMP2 levels are highly expressed in the BLM group due to lung fibrosis.

Likewise, the current study revealed that BLM installation was associated with a significant increase in Caspase-3 gene expression and MUC5AC in lung tissue homogenates. This was accompanied by a profound decrease in BCL-2 gene expression in lung tissue after 14 and 28 days of study in the BLM group when compared to the NC group. These results suggest that the overexpression of caspase-3 may reflect the up-regulation of the apoptosis pathway in alveolar and bronchiolar epithelial cells associated with pulmonary fibrosis [49,50].

The enhanced expression of the MUC5AC gene present in this study under BLM installation confirms the mucus hypersecretion in acute lung damage. This might be due to goblet cell hyperplasia and mucin overproduction in this model. This may be also related to the activating role of neutrophil-derived products such as ROS and the enhanced production of TNF-α [51] the histological study and the grades of lung fibrosis of lung tissue sections stained by H&E and Masson trichrome stain aimed to support the biochemical investigations.

Furthermore, the histological examination of lung sections of the BLM group of the present study revealed various changes such as many collapsed alveoli, while other alveoli were dilated and ruptured. Some bronchioles were lined by epithelial cells with deeply stained nuclei and its lumen was full of exfoliated epithelial cells. Also, heavy mononuclear cellular infiltration surrounding the bronchioles and in the interalveolar septa were present. The dilated and congested blood vessels and interstitial hemorrhage in the alveolar spaces were seen.

Moreover, a significant increase in the amount of collagen and elastic fibers around the bronchiole and the walls of the alveoli. Additionally, BLM was associated with diffuse mononuclear cellular infiltration surrounding the bronchioles and the interalveolar septa with diffused thickening of the interalveolar septa [52].

Besides, **Ashcroft** *et al.* [30] and **Zhou** *et al.* [31], developed a numerical scale for determining the degree of fibrosis in lung specimens. This scale was applied here in this study in all experimental groups. In the present study, histological alterations in mice lung section following 14 days of BLM installation were manifested in the form of early fibrosis and inflammatory cell aggregates with increased grade 7 fibrosis at 28 days. This may be related to the activated inflammatory cells and fibroblasts that can synthesize and secrete reactive oxygen species, various chemokines, and cytokines, and proteases, which can lead to aberrant fibro proliferation and collagen production and deposition in lung tissues of mice with interalveolar septal thickening, accumulation of exudative fluids in alveolar space, diffuse infiltration of lymphocytes, neutrophils, and macrophages in BAL fluid [53].

Treatment with DEX alone or DEX loaded on NCs particles to BLM induced lung fibrotic mice for 14 and 28 days induced a significant decline *(p < 0.05)* in serum LDH and MDA, tissue hydroxyproline, and collagen 1α. This was also accompanied by a decrease in the inflammatory mediators including TNF-α, TGF-β1, NFκB, and lung tissue inflammatory marker MMP2. These results were followed by a decrease in the gene expression of Caspase-3 and MUC5AC genes and a significant increase in the BCL2 gene in lung tissue when compared to the BLM group. In addition, the microscopical investigation of the total leukocyte count and the differential counts of macrophage, lymphocytes, and neutrophils in BAL fluid revealed likewise a significant decrease under treatment with DEX alone or DEX loaded on NCs particles. The more ameliorated results were established in the BLM group of mice that was treated with DEX–NCs. These results were confirmed by the histological examination of lung tissue sections diminishing the fibrotic graded scale from grade 7 in the BLM group to grade 4 after applying DEX-NCs treatment. This may be due to the relative stability of DEX-NCs particles under physiological conditions. When nanoparticles reached the pathological site or are taken up into the lysosome by the cells, DEX is rapidly released from its Nanocarrier to further exert its pharmacological effects. Also, loading DEX onto NCs particles could have increased the retention rate of the drug in the circulatory system and reduced its clearance. This might be advantageous to the targeting of nanoparticles, providing evidence for the possibility of low-dose administration or prolonged dosing intervals of nanoparticles [54].

DEX treatment to BLM-induced lung injury model failed to reduce the neutrophil infiltration in BAL fluid along with lung edema and lung injury scores. Additionally, neither cellular infiltration nor cytokine release was inhibited by DEX treatment alone. This might be related to the damaging effect of DEX on the repair capacity of the alveolar epithelium [55].

More to the point, these results highlight the effectiveness of the investigated DEX-NCs particles because loading DEX onto NCs particles potently accumulated in macrophages, upon administration and improved the delivery and release of DEX to target lung cells and tissues [56]. The novel formulation DEX-NCs efficiently targeted the pulmonary macrophages and improved PF as compared to DEX treatment. DEX-NCs suppressed inflammatory cytokines. In addition, DEX-NCs targeted DEX to myeloid and lymphoid tissues that were enriched with phagocytes. It also enabled efficient and relatively selective delivery of the potent corticosteroid drug to sites of inflammation where the vasculature was leaky and where large numbers of phagocytes had infiltrated, thus attenuating the production of proinflammatory cytokines and other signaling molecules that contribute to edema formation and progressive lung tissue damage [57]. Also, **Wang and Sun** [58] verified that inflamed tissues possess enhanced vascular permeability, so Nanocarriers could extravasate into the inflamed sites. Then, inflammatory cells in the inflamed areas seize Nanocarriers between 10 and 200 nm to the target inflammatory sites alleviating the inflammatory symptoms with a lower dose and decrease the adverse effects of DEX on body tissues. Likewise, DEX-NCs might sustain the release of DEX to act as an anti-inflammatory and anti-edema drug in the site of inflammation for a longer duration to cure pulmonary fibrosis completely [59].

In line with the results of the present study, **Jia et al.** [60] indicated that both treatments of DEX and DEX-NCs down-regulated the elevated levels of inflammatory mediators and markers in the BLM group. There was an increased therapeutic efficacy in DEX-NCs than the DEX group which could be attributed to the superior drug targeting characteristic and higher bioavailability and sustained drug release in the inflamed site [57].

Again DEX-NCs treatment in the PF mice model reduced hydroxyproline content when compared to BLM PF mice, especially the DEX-NCs group, suggesting the role of DEX in inhibiting fibrosis induced by BLM treatment via inhibition of collagen synthesis and preventing its structure formation [61]. This may be achieved by decreasing inflammatory cell migration and proliferation. DEX directly suppressed fibroblasts and decreased the transcription of type I procollagen mRNA in the fibroblast, thus suppressing collagen synthesis. Likewise, DEX reduced hydroxyproline with a reduction in the extracellular matrix and collagen deposition [62, 63].

The anti-inflammatory effect of DEX is exerted through binding to the intracellular glucocorticoid receptor thereafter to specific DNA sequences such as IκBα which is the gatekeeper that limits NFκB migration into the nucleus andthem in an inactive state in the cytoplasm. Furthermore, NFκB regulates the transcription of an array of cytokine genes, including TNF-α [64, 65].

The histological examination of lung sections of BLM groups that were treated with DEX and DEX-NCs in the present study revealed some collapsed alveoli. Moreover, a significant decrease in collagen and elastic fibers around alveoli and within the interalveolar septa and around bronchioles was evident in these groups with evident ameliorated lung tissue sections after 28 days of DEX-NCs treatment. These results were in agreement with **Zhou et al.** [8] who proved that dexamethasone can attenuate BLM-induced lung injury by down modulating the inflammatory responses, secretion of pro-inflammatory cytokines, and ameliorating fibrosis.

5. Research limitations

Dexamethasone nano-chitosan particles decreased significantly lung tissue inflammatory mediators, collagen profile. Further studies of the cellular and hormonal effects of dexamethasone Nano chitosan particles on different organs must be made to confirm the efficacy of this Nano particle.

6. Conclusion

Loading dexamethasone onto Nano chitosan particles synthesized from chitosan has shown improved pharmacokinetics of dexamethasone and provided novel insights in pulmonary injury treatment.

Disclosure statement

No potential conflict of interest was reported by the authors.

ORCID

Afaf Hendawy Kamel http://orcid.org/0000-0002-2003-1889
Waleed Khaled. El Zawawy http://orcid.org/0000-0003-0216-2081
Nashwa Ahmed El-shinawy http://orcid.org/0000-0001-6945-3479

References

[1] Chen C, Wang Y-Y, Wang Y-X, et al. Gentiopicroside ameliorates bleomycin-induced pulmonary fibrosis in mice via inhibiting inflammatory and fibrotic process. Biochem Biophys Res Commun. 2018;495 (4):2396–2403.

[2] El-Khoury D, El-Bakly WM, Awad AS, et al. Thymoquinone blocks lung injury and fibrosis by attenuating bleomycin-induced oxidative stress and activation of nuclear factor Kappa-B in rats. Toxicology. 2012;302(2–3):106–113.

[3] Pereyra BBS, Freitas MM, Almeida DD. New access of pulmonary fibrosis induced by bleomycin in rats. Int J Dev Res. 2018;8(3):19271–19275.

[4] Liu J-F, Nie X-C, Shao Y-C, et al. Bleomycin suppresses the proliferation and the mobility of human gastric cancer cells through the smad signaling pathway. Cell Physiol Biochem. 2016;40(6):1401–1409.

[5] Williamson JD, Sadofsky LR, Crooks MG, et al. Bleomycin increases neutrophil adhesion to human vascular endothelial cells independently of upregulation of ICAM-1 and E-selectin. Exp Lung Res. 2016;42(8–10):397–407.

[6] Rajasekaran S, Rajaguru P, Sudhakar Gandhi PS. MicroRNAs as potential targets for progressive pulmonary fibrosis. Front Pharmacol. 2015;6(254). DOI:10.3389/fphar.2015.00254

[7] Shi K, Jiang J, Ma T, et al. Dexamethasone attenuates bleomycin-induced lung fibrosis in mice through TGF-β, Smad3 and JAK-STAT pathway. Int J Clin Exp Med. 2014;7(9):2645.

[8] Zhou Y, Liao S, Wang B, et al. Dexamethasone suppresses bleomycin-induced pulmonary fibrosis via down-regulation of jagged1/notch1 signaling pathway. Int J Clin Exp Med. 2016;9(2):2897–2904.

[9] Ramamoorthy S, Cidlowski JA. Corticosteroids: mechanisms of action in health and disease. Rheum Dis Clin. 2016;42(1):15–31.

[10] Cruz-Topete D, Cidlowski JA. One hormone, two actions: anti-and pro-inflammatory effects of glucocorticoids. Neuroimmunomodulation. 2015;22 (1–2):20–32.

[11] Wu D-Y, Ou C-Y, Chodankar R, et al. Distinct, genome-wide, gene-specific selectivity patterns of four glucocorticoid receptor coregulators. Nucl Recept Signal. 2014;12(1):nrs. 12002. https://doi.org/10.1621%2Fnrs.12002

[12] Han Y, Han L, Dong M, et al. Comparison of a loading dose of dexmedetomidine combined with propofol or sevoflurane for hemodynamic changes during anesthesia maintenance: a prospective, randomized, double-blind, controlled clinical trial. BMC Anesthesiol. 2018;18(1):12.

[13] Oray M, Samra KA, Ebrahimiadib N, et al. Long-term side effects of glucocorticoids. Expert Opin Drug Saf. 2016;15(4):457–465.

[14] Khalid M, El-Sawy HS. Polymeric nanoparticles: promising platform for drug delivery. Int J Pharm. 2017;528(1–2):675–691.

[15] Todoroff J, Vanbever R. Fate of nanomedicines in the lungs. Curr Opin Colloid Interface Sci. 2011;16 (3):246–254.

[16] Ramezani Z, Zarei M, Raminnejad N. Comparing the effectiveness of chitosan and nanochitosan coatings on the quality of refrigerated silver carp fillets. Food Control. 2015;51:43–48.

[17] Shanmuganathan R, Edison TNJI, LewisOscar F, et al. Chitosan nanopolymers: an overview of drug delivery against cancer. Int J Biol Macromol. 2019;130:727–736.

[18] Rizvi SA, Saleh AM. Applications of nanoparticle systems in drug delivery technology. Saudi Pharm J. 2018;26(1):64–70.

[19] Ghadi A, Mahjoub S, Tabandeh F, et al. Synthesis and optimization of chitosan nanoparticles: potential applications in nanomedicine and biomedical engineering. Caspian J Intern Med. 2014;5 (3):156–161.

[20] Stelte W, Sanadi AR. Preparation and characterization of cellulose nanofibers from two commercial hardwood and softwood pulps. Ind Eng Chem Res. 2009;48(24):11211–11219.

[21] Hu Z, Zhai R, Li J, et al. Preparation and characterization of nanofibrillated cellulose from bamboo fiber via ultrasonication assisted by repulsive effect. Int J Polym Sci. 2017;2017:1–9.

[22] Paget G, Barnes J. Toxicity tests, evaluation of drug activities: pharmacometrics. British Medical Journal. 1964;1:135–165.

[23] Ellefson R, Caraway W. Fundamentals of clinical chemistry. 1976. Ed Tietz NW 506.

[24] Kei S. Serum lipid peroxide in cerebrovascular disorders determined by a new colorimetric method. Clin Chim Acta. 1978;90(1):37–43.

[25] Pfaffl MW. A new mathematical model for relative quantification in real-time RT–PCR. Nucleic Acids Res. 2001;29(9):e45–e45.

[26] Sun F, Xiao G, Qu Z, et al. Murine Bronchoalveolar Lavage. Bio-protocol. 2017;7(10):e2287.

[27] Kimura T, Nojiri T, Hosoda H, et al. Exacerbation of bleomycin-induced injury by lipopolysaccharide in mice: establishment of a mouse model for acute exacerbation of interstitial lung diseases. Eur J Cardiothorac Surg. 2015;48(4):e85–91.

[28] Bancroft JD, Cook HC. Manual of histological techniques and their diagnostic application. Churchill Livingstone; 1994.

[29] Puchtler H, Waldrop FS, Conner H, et al. Carnoy fixation: practical and theoretical considerations. Histochemie. 1968;16(4):361–371.

[30] Ashcroft T, Simpson JM, Timbrell V. Simple method of estimating severity of pulmonary fibrosis on a numerical scale. J Clin Pathol. 1988;41 (4):467–470.

[31] Zhou Y, Huang X, Hecker L, et al. Inhibition of mechanosensitive signaling in myofibroblasts ameliorates experimental pulmonary fibrosis. J Clin Investig. 2013;123(3):1096–1108.

[32] De Langhe E, Cailotto F, De Vooght V, et al. Enhanced endogenous bone morphogenetic protein signaling protects against bleomycin induced pulmonary fibrosis. Respir Res. 2015;16(1):1–10.

[33] Raghu G. Pharmacotherapy for idiopathic pulmonary fibrosis: current landscape and future potential. Eur Respir Rev. 2017;26(145):170071.

[34] Asker SA, Mazroa SA, Boshra V, et al. Biochemical and histological impact of direct renin inhibition by aliskiren on myofibroblasts activation and differentiation in bleomycin induced pulmonary fibrosis in adult mice. Tissue Cell. 2015;47(4):373–381. https://doi.org/10.1016/j.tice.2015.05.001

[35] Walters DM, Kleeberger SR. Mouse models of bleomycin-induced pulmonary fibrosis. Curr Protoc Pharmacol. 2008;40(1):5.46. 1–5.46. 17.

[36] Quan L, Zhang Y, Dusad A, et al. The evaluation of the therapeutic efficacy and side effects of a macromolecular dexamethasone prodrug in the collagen-induced arthritis mouse model. Pharm Res. 2016;33(1):186–193.

[37] Suke SG, Negi H, Mediratta P, et al. Anti-arthritic and anti-inflammatory activity of combined pioglitazone and prednisolone on adjuvant-induced arthritis. Eur J Pharmacol. 2013;718(1–3):57–62.

[38] Kar S, Konsam S, Hore G, et al. Therapeutic use of fisetin, curcumin, and mesoporous carbaon nanoparticle loaded fisetin in bleomycin-induced idiopathic pulmonary fibrosis. Biomed Res Ther. 2015;2 (4):250–262.

[39] Yang X, Wu L, Li G, et al.Alphacalcidol combined with dexamethasone for reducing pulmonary fibrosis in mice and its mechanism. Chin J Cell Mol Immunol= Xi Bao Yu Fen Zi Mian Yi Xue Za Zhi. 2017;33(4):488–491PMID: 28395719.

[40] Cánepa C, Imperiale JC, Berini CA, et al. Development of a drug delivery system based on Chitosan nanoparticles for oral administration of Interferon-α. Biomacromolecules. 2017;18 (10):3302–3309. https://doi.org/10.1021/acs.biomac. 7b00959

[41] Bakhsheshi-Rad H, Hadisi Z, Ismail A, et al. In vitro and in vivo evaluation of chitosan-alginate/gentamicin wound dressing nanofibrous with high antibacterial performance. Polym Test. 2020;82:106298.

[42] Chen H, Zhang J, Hao H, et al. Hydrogen-rich water increases postharvest quality by enhancing antioxidant capacity in Hypsizygus marmoreus. AMB Express. 2017;7(1):221.

[43] Kseibati MO, Shehatou GSG, Sharawy MH, et al. Nicorandil ameliorates bleomycin-induced pulmonary fibrosis in rats through modulating eNOS, iNOS, TXNIP and HIF-1α levels. Life Sci. 2020;246:117423.

[44] Joshi S, Singh AR, Wong SS, et al. Rac2 is required for alternative macrophage activation and bleomycin induced pulmonary fibrosis; a macrophage autonomous phenotype. PloS One. 2017;12(8):e0182851. https://doi.org/10.1371/journal.pone.0182851

[45] Zhou Z, Kandhare AD, Kandhare AA, et al. Hesperidin ameliorates bleomycin-induced experimental pulmonary fibrosis via inhibition of TGF-beta1/Smad3/AMPK and IkappaBalpha/ NF-kappaB pathways. EXCLI J. 2019;18:723.

[46] Li L-C, Li D-L, Xu L, et al. High-mobility group box 1 mediates epithelial-to-mesenchymal transition in pulmonary fibrosis involving transforming growth factor-β1/Smad2/3 signaling. J Pharmacol Exp Ther. 2015;354(3):302–309.

[47] Reinert T, Baldotto CSDR, Nunes FAP, et al. Bleomycin-induced lung injury. J Cancer Res. 2013;2013:9.

[48] Bradding P, Pejler G. The controversial role of mast cells in fibrosis. Immunol Rev. 2018;282(1):198–231.

[49] Delbridge A, Strasser A. The BCL-2 protein family, BH3-mimetics and cancer therapy. Cell Death Differ. 2015;22(7):1071–1080.

[50] Tian F, Fu X, Gao J, et al. Caspase-3 mediates apoptosis of striatal cells in GA I rat model. J Huazhong Univ Sci Technol. 2012;32(1):107–112.

[51] Thimmulappa RK, Chattopadhyay I, Rajasekaran S. Oxidative stress mechanisms in the pathogenesis of environmental lung diseases. In: Oxidative stress in lung diseases. Springer; 2020. 103–137. https://doi. org/10.1007/978-981-32-9366-3

[52] Gilhodes J-C, Julé Y, Kreuz S, et al. Quantification of pulmonary fibrosis in a bleomycin mouse model using automated histological image analysis. PloS One. 2017;12(1):e0170561. https://doi.org/10.1371/ journal.pone.0170561

[53] Tashiro J, Rubio GA, Limper AH, et al. Exploring animal models that resemble idiopathic pulmonary fibrosis. Front Med. 2017;4:118.

[54] Liu H, Zhang H, Yin N, et al. Sialic acid-modified dexamethasone lipid calcium phosphate gel core nanoparticles for target treatment of kidney injury. Biomater Sci. 2020. DOI:10.1039/D0BM00581A

[55] Aubin Vega M, Chupin C, Pascariu M, et al. Dexamethasone fails to improve bleomycin-induced acute lung injury in mice. Physiol Rep. 2019;7(21): e14253.

[56] Ledford H. Coronavirus breakthrough: dexamethasone is first drug shown to save lives. Nature. 2020;582(7813):469.

[57] Zhang J, Leifer F, Rose S, et al. Amikacin liposome inhalation suspension (ALIS) penetrates non-tuberculous mycobacterial biofilms and enhances amikacin uptake into macrophages. Front Microbiol. 2018;9:915.

[58] Wang Q, Sun X. Recent advances in nanomedicines for the treatment of rheumatoid arthritis. Biomater Sci. 2017;5(8):1407–1420.

[59] Lammers T, Sofias AM, van der Meel R, et al. Dexamethasone nanomedicines for COVID-19. Nat Nanotechnol. 2020;15(8):622–624.

[60] Jia M, Deng C, Luo J, et al. A novel dexamethasone-loaded liposome alleviates rheumatoid arthritis in rats. Int J Pharm. 2018;540(1– 2):57–64.

[61] Durmus M, Karaaslan E, Ozturk E, et al. The effects of single-dose dexamethasone on wound healing in rats. Anesth Analg. 2003;97(5):1377–1380.

[62] Raish M, Ahmad A, Ahmad Ansari M, et al. Sinapic acid ameliorates bleomycin-induced lung fibrosis in rats. Biomed Pharmacother. 2018;108:224–231.

[63] Li X, Wu Z, An X, et al. Blockade of the LRP16-PKR-NF-κB signaling axis sensitizes colorectal carcinoma cells to DNA-damaging cytotoxic therapy. Elife. 2017;6:e27301.

[64] Dustgania A, Vasheghani Farahani E, Imani M. Preparation of Chitosan nanoparticles loaded by Dexamethasone Sodium Phosphate. Iran J Pharm Sci. 2008;4(2):111–114.

[65] Tang P, Sun Q, Zhao L, et al. Mesalazine/hydroxypropyl-β-cyclodextrin/chitosan nanoparticles with sustained release and enhanced anti-inflammation activity. Carbohydr Polym. 2018;198:418–425.